

# Synthesis, Structure, and Luminescence of 2D-Dilute Magnetic Semiconductors: $\text{Zn}_{1-x}\text{Mn}_x\text{Se} \cdot 0.5\text{L}$ (L = Diamines)

Jun Lu, Shuo Wei, Yiya Peng, Weichao Yu, and Yitai Qian\*

Structure Research Laboratory, and Department of Chemistry, University of Science and Technology of China, Hefei, Anhui 230026, P.R. China

Received: August 14, 2002; In Final Form: November 19, 2002

The two-dimension dilute magnetic semiconductors (2D-DMS)  $\text{Zn}_{1-x}\text{Mn}_x\text{Se} \cdot 0.5\text{L}$  (L = ethylenediamine or en, 1,3-propanediamine or pda, 1,4-butanediamine or bda, and 1,6-hexanediamine or hda) and their host compounds  $\text{ZnSe} \cdot 0.5\text{L}$  were prepared by solvothermal reaction in solvent L at 190 °C. The powder X-ray diffraction patterns of  $\text{ZnSe} \cdot 0.5\text{L}$  are indexed as isomorphous orthorhombic lattices, whose constants  $c$  increase monotonically from L = en to L = hda. The orthorhombic lattice in  $ab$  plane of  $\text{ZnSe} \cdot 0.5\text{en}$  is a shrunken 2D superlattice ( $\sqrt{3}a \times c$ ) of the (110) plane of hexagonal ZnSe. When  $\text{Zn}^{2+}$  is partly substituted by  $\text{Mn}^{2+}$ ,  $\text{Zn}_{1-x}\text{Mn}_x\text{Se} \cdot 0.5\text{L}$  become 2D-DMS. Their photoluminescence (PL) spectra show strong  $\text{Mn}^{2+}$ -related emission peaks at 2.07 eV (600 nm). The Mn content dependence of PL intensity of  $\text{Zn}_{1-x}\text{Mn}_x\text{Se} \cdot 0.5\text{hda}$  is especially studied, and high intensities are obtained when  $x < 0.2$ . For  $x \approx 0.2$ , the PL intensities of  $\text{Zn}_{1-x}\text{Mn}_x\text{Se} \cdot 0.5\text{L}$  increase from L = en to L = hda, which can be attributed to the formation of Zn/Mn–N bonds and the effective energy transfer routes and radiative recombination of the 3d electron of  $\text{Mn}^{2+}$  within the 2D  $[\text{Zn}_{1-x}\text{Mn}_x\text{Se}]$  layers.

## 1. Introduction

Mn-based II–VI group compounds have been extensively studied as typical diluted magnetic semiconductors (DMS). They have wide direct gaps and outstanding magneto-optical properties such as strong Faraday rotation and giant exciton Zeeman splitting,<sup>1–3</sup> which originate from the s,p-d exchange interaction between band electron/hole and  $\text{Mn}^{2+}$  3d<sup>5</sup> electron.<sup>4–7</sup> These properties make it possible to fabricate high performance microstructures of optoelectronic devices. In the past two decades, the optical properties of 2D  $\text{Zn}_{1-x}\text{Mn}_x\text{Se}$  quantum wells and superlattices grown by molecular beam epitaxy (MBE) have been researched.<sup>8–11</sup> Recently, the  $\text{Mn}^{2+}$ -related emission ( $^4\text{T}_1 \rightarrow ^6\text{A}_1$ ) with high quantum efficiency was obtained in  $\text{Zn}_{1-x}\text{Mn}_x\text{Se}$  nanocrystals and quantum dots.<sup>12, 13</sup>

Inorganic/organic (I/O) hybrid compounds have novel properties due to the combination of inorganic components and organic molecules. The diamine-intercalated layered compounds,  $\text{ZnE} \cdot 0.5\text{L}$ ,  $\text{MnSe} \cdot 0.5\text{L}$  and  $\text{Zn}_{1-x}\text{Mn}_x\text{Se} \cdot 0.5\text{L}$  (E = Se, Te, and L = en, pda), which were solvothermally synthesized,<sup>14</sup> are a novel type of the I/O hybrid structures. Optical absorption measurements show that the band gaps of  $\text{ZnSe} \cdot 0.5\text{L}$  and  $\text{Zn}_{1-x}\text{Mn}_x\text{Se} \cdot 0.5\text{L}$  have large blue shifts (1.4–1.5 eV) compared with that of ZnSe,<sup>15,16</sup> which are attributed to the quantum confinement effect of the  $[\text{Zn}_{1-x}\text{Mn}_x\text{Se}]$  layers.

In this study,  $\text{ZnSe} \cdot 0.5\text{L}$  and 2D-DMS  $\text{Zn}_{1-x}\text{Mn}_x\text{Se} \cdot 0.5\text{L}$  (L = en, pda, bda, and hda) were synthesized by solvothermal reaction in solvent L at 190 °C. The indexing of the powder XRD patterns of  $\text{ZnSe} \cdot 0.5\text{L}$  indicates that they are isomorphous crystals. The structural relationship between  $\text{ZnSe} \cdot 0.5\text{en}$  and hexagonal ZnSe are revealed. In the PL spectra,  $\text{Zn}_{1-x}\text{Mn}_x\text{Se} \cdot 0.5\text{L}$  shows strong  $\text{Mn}^{2+}$ -related emission at 2.07 eV (600 nm). The high PL intensities can be obtained when the Mn content ( $x$ ) is

less than 0.2 according to the Mn content dependence of the PL intensity of  $\text{Zn}_{1-x}\text{Mn}_x\text{Se} \cdot 0.5\text{hda}$ . For  $\text{Zn}_{1-x}\text{Mn}_x\text{Se} \cdot 0.5\text{L}$  ( $x \approx 0.2$ ), the luminescence-enhancement effect is observed.

## 2. Experimental Section

**2.1. Synthesis.** 1,3-Propanediamine (pda, 99%) and 1,4-butanediamine (bda, 98%) were purchased from Fluka Chemicals Co. Ltd. Other chemicals were of analytical grade purity and were purchased from Shanghai Chemical Reagent Co. Ltd.

$\text{ZnSe} \cdot 0.5\text{L}$  (L = en, pda, bda, and hda) were solvothermally synthesized as follows. A 5 mmol sample of  $\text{Zn}(\text{CH}_3\text{CO}_2)_2 \cdot 2\text{H}_2\text{O}$  and 5 mmol of selenium were dissolved into 50 mL of solvent L. The mixture was sealed into a 60 mL Teflon-lined stainless steel autoclave, heated at 190 °C for 7 days, and then cooled naturally. The products were washed with distilled water and absolute ethanol and then dried in a vacuum at 70 °C for 2 h.  $\text{Zn}_{1-x}\text{Mn}_x\text{Se} \cdot 0.5\text{L}$  were prepared in a similar procedure with different molar ratios of  $\text{Zn}^{2+}:\text{Mn}^{2+}$  ( $\text{Mn}(\text{CH}_3\text{CO}_2)_2 \cdot 4\text{H}_2\text{O}$  as Mn source).

**2.2. Component Analysis.** Elemental analysis of C, H, and N weight percentages of  $\text{ZnSe} \cdot 0.5\text{L}$  (using a Perkin-Elmer 2400 elemental analyzer) are listed in Table 1. It can be seen that the obtained data of H and N are consistent with the calculated values in the range of experimental error ( $\pm 0.5\%$ ). As for C, however, the slightly greater experimental values probably resulted from the carbon contamination of sample surfaces. Therefore, the chemical stoichiometry of  $\text{ZnSe} \cdot 0.5\text{L}$  can be regarded as accurate.

Inductively coupled plasma-atomic emission spectra (ICP-AES, using an Atomscan Advantage Spectrometer, Thermo Jarrell Ash Corp.) were used to determine the Mn contents of  $\text{Zn}_{1-x}\text{Mn}_x\text{Se} \cdot 0.5\text{L}$ . For L = hda,  $\text{Zn}^{2+}:\text{Mn}^{2+} = 19:1, 9:1, 7:3, 3:2, 2:3$ , and  $1:4$ , the determined Mn contents are  $x = 0.046, 0.0829, 0.279, 0.390, 0.581$ , and  $0.779$ , respectively. For  $\text{Zn}^{2+}:$

\* Corresponding author. Fax: (+86) 0551-3607402. E-mail: ytqian@ustc.edu.cn.

TABLE 1: Analysis Results of C, H, and N Contents of ZnSe·0.5L

	C, H, N (wt %)			
	L = en	L = pda	L = bda	L = hda
calcd	9.42, 3.16, 10.99	9.93, 2.778, 7.721	12.75, 3.206, 7.433	17.80, 3.978, 6.918
found	9.77, 3.02, 11.10	11.35, 2.791, 7.995	13.66, 3.254, 7.409	18.57, 3.980, 6.902

TABLE 2: Indexing Results of Powder X-ray Diffraction of ZnSe·0.5L

L	cryst			vol (Å <sup>3</sup> )	program	FOM
	syst	a (Å)	b (Å)			
en	ortho	6.634	6.459	17.360	ITO15	$M_{20} = 26.0$
pda	ortho	6.638	6.450	20.010	ITO15	$M_{20} = 58.9$
bda	ortho	6.610	6.446	22.188	DICVOL91	$F_{19} = 8.8$
hda	ortho	6.616	6.449	27.116	DICVOL91	$F_{24} = 16.6$

$\text{Mn}^{2+} = 4:1$  with different L, the determined Mn contents are  $x = 0.159$  (L = en),  $x = 0.173$  (L = pda),  $x = 0.205$  (L = bda), and  $x = 0.195$  (L = hda), respectively. Therefore, the synthetic reactions for  $\text{Zn}^{2+}:\text{Mn}^{2+}$  varying from 19:1 to 1:4 can be regarded as quantitative.

**2.3. Indexing of Powder XRD Patterns of ZnSe·0.5L.** The powder XRD patterns of ZnSe·0.5L ( $2\theta$ : 5.00–65.00°) were collected using a MAX 18 AHF X-ray diffractometer (MAC Science Co. Ltd., Cu  $K\alpha_1$ ,  $\lambda = 1.54056$  Å, scanning rate 8.0000°  $\text{min}^{-1}$ ). Indexing and lattice constant refinements were carried out by three PC software programs ITO15,<sup>17</sup> TRERRO90,<sup>18,19</sup> and DICVOL91,<sup>20,21</sup> and the  $2\theta$  values of selected well-defined diffraction peaks were used as input data. The results are compared and the most reliable ones are listed in Table 2, which give consistent orthorhombic lattices with good figures of merit (FOM,  $M_N$  and  $F_N$ , simplified criteria for the reliability of a powder diffraction indexing<sup>22–24</sup>). The indexed constants of ZnSe·0.5en and ZnSe·0.5pda are consistent with the reported values,<sup>15</sup> those of ZnSe·0.5bda and ZnSe·0.5hda are not reported previously. It can be seen that the indexed constants  $a$  and  $b$  in all of the four compounds are almost identical, which implies that the 2D [ZnSe] layer structure in L = en and pda<sup>15</sup> is preserved in L = bda and hda. The increase of the  $c$  axis from L = en (17.360 Å) to L = hda (27.116 Å) is reasonably parallel with the lengthening of diamine molecules from en to hda.

**2.4. Photoluminescence Measurement.** The PL emission and excitation spectra of  $\text{Zn}_{1-x}\text{Mn}_x\text{Se} \cdot 0.5\text{L}$  were recorded at room temperature with a Hitachi 850 fluorescence spectrophotometer. The measurement conditions were identical in all cases and therefore relative intensities can be compared.

### 3. Results and Discussion

**3.1. Structural Relationship of ZnSe·0.5en and Hexagonal ZnSe.** Comparing with hexagonal ZnSe, one finds that the size of the orthorhombic lattice in the  $ab$  plane of ZnSe·0.5en ( $6.633 \times 6.463$  Å) is close to that of the  $\sqrt{3}a \times c$  orthorhombic lattice ( $6.921 \times 6.53$  Å) in the (110) plane of hexagonal ZnSe (JCPDS, PDF, 15-105). Therefore, the unit cell in the  $ab$  plane of ZnSe·0.5en can be viewed as a shrunken  $\sqrt{3}a \times c$  2D superlattice of the (110) plane of hexagonal ZnSe. It can be expected that the coordination of  $\text{Zn}^{2+}$  in ZnSe·0.5en should be similar to the  $\text{ZnSe}_4$  tetrahedra in hexagonal ZnSe. This has been verified by the crystallographic analysis of ZnSe·0.5en polycrystals and its isomorphous one-MnSe·0.5en single crystal.<sup>15</sup> The structure of ZnSe·0.5en is shown in Figure 1 where the  $\text{ZnSe}_4$  coordination tetrahedra are revealed. On the other hand, when ethylenediamine molecules are removed from ZnSe·0.5en by acid washing or annealing at elevated temperature,<sup>25</sup> lamellar hexagonal ZnSe crystallites with (110) orientation are obtained. Taking the above

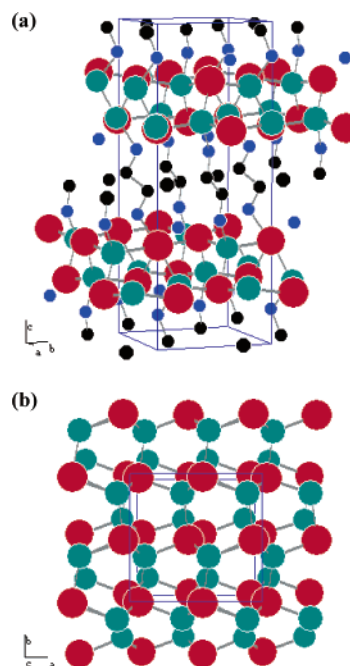


**Figure 1.** View of the structure of ZnSe·0.5en along the  $a$  axis (a, top) and along the  $c$  axis (b, bottom). Green (middle) circles are Zn, red (large) circles are Se, black and blue (small) circles are C and N, respectively; the unit cell was outlined as well. The atomic coordinates in ref 15 were cited in this figure.

analyses into consideration, this deintercalation reaction can be described as follows, when diamine molecules leave the lattice, Zn–N bonds are broken, 2D [ZnSe] monolayers collapse along the  $c$  axis, and the fourth Zn–Se bonds form, which result in hexagonal ZnSe crystallites with (110) cleavage. Therefore, it can be concluded that the deintercalation reaction is topochemical. Because ZnSe·0.5en and MnSe·0.5en are isomorphous crystals, their solid solution of  $\text{Zn}_{1-x}\text{Mn}_x\text{Se} \cdot 0.5\text{L}$  can be consequently regarded as 2D-DMS.

**3.2. Mn Content Dependence of PL Intensities of  $\text{Zn}_{1-x}\text{Mn}_x\text{Se} \cdot 0.5\text{hda}$ .** Figure 3d shows the PL spectra of the as-prepared  $\text{Zn}_{1-x}\text{Mn}_x\text{Se} \cdot 0.5\text{hda}$  ( $x = 0.195$ ), where a strong emission peak at 595–600 nm can be seen. The Mn content dependence of this PL emission intensity is shown in Figure 2. The monotonically decreasing curve indicates that, in the range of low Mn content ( $x < 0.2$ ), high intensities are obtained. In our experiments, the maximal intensity appears at  $x = 0.046$ . When  $x > 0.4$ , the intensity decreases to about 10% of the maximum, and when  $x = 0.8$ , only 5% exists. In the excitation spectra of  $\text{Zn}_{1-x}\text{Mn}_x\text{Se} \cdot 0.5\text{hda}$  (not shown), sharp peaks with a slight blue shift (from 300 nm ( $x = 0.046$ ) to 291 nm ( $x = 0.779$ )) are found, which may result from the structural distortion of  $\text{Zn}_{1-x}\text{Mn}_x\text{Se} \cdot 0.5\text{hda}$  due to  $\text{Mn}^{2+}$  substitution.

**3.3. Luminescence-Enhancement Effect of  $\text{Zn}_{1-x}\text{Mn}_x\text{Se} \cdot 0.5\text{L}$  ( $x \approx 0.2$ ).** Figure 3 shows the PL excitation (left) and emission (right) spectra of the isomorphous  $\text{Zn}_{1-x}\text{Mn}_x\text{Se} \cdot 0.5\text{L}$  ( $x \approx 0.2$ ). All have emission peaks at 2.07 eV (595–600 nm) with a half-width of 0.24 eV. In the excitation spectra, the sharp peaks at 4.09 eV (303 nm) for L = en and 4.16 eV (298 nm) for L = pda (also bda and hda) reflect their band gaps and are both

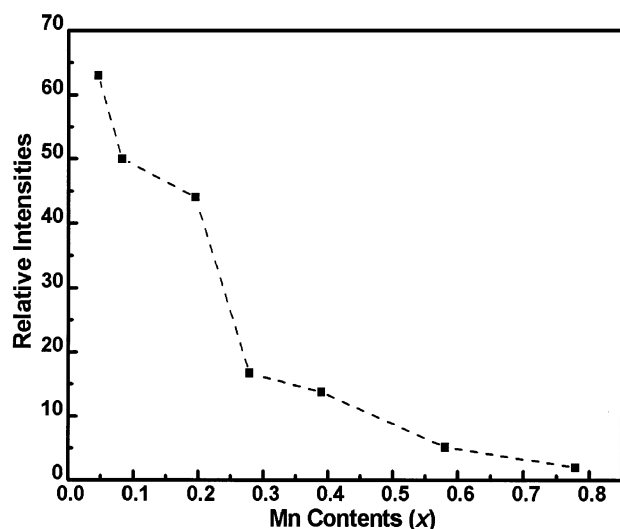


Figure 2. Mn content dependence of PL intensities of  $\text{Zn}_{1-x}\text{Mn}_x\text{Se} \cdot 0.5\text{hda}$ .

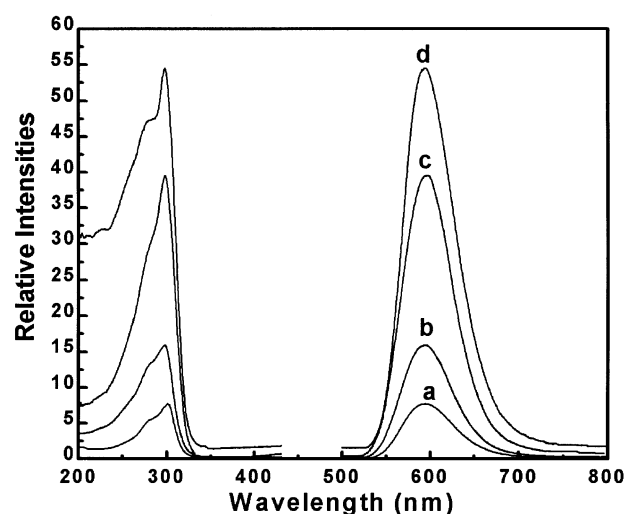


Figure 3. PL excitation and emission spectra of  $\text{Zn}_{1-x}\text{Mn}_x\text{Se} \cdot 0.5\text{L}$  ( $x \approx 0.2$ ): (a)  $\text{L} = \text{en}$ ; (b)  $\text{L} = \text{pda}$ ; (c)  $\text{L} = \text{bda}$ ; (d)  $\text{L} = \text{hda}$ .

greater than the estimated values of 4.0 eV ( $\sim 310$  nm) and 3.9 eV (318 nm) from optical absorption spectra,<sup>15</sup> respectively. Therefore, the excitation for 2.07 eV emission originates from a band–band transition of a ZnSe host like traditional  $\text{Zn}_{1-x}\text{Mn}_x\text{Se}$  DMS. Compared with the emission at 2.12 eV (585 nm) of bulk  $\text{Zn}_{1-x}\text{Mn}_x\text{Se}$ ,<sup>26,27</sup> the emission peaks of  $\text{Zn}_{1-x}\text{Mn}_x\text{Se} \cdot 0.5\text{L}$  ( $x \approx 0.2$ ) can be assigned to the  $\text{Mn}^{2+}$  internal transition ( ${}^4\text{T}_1 \rightarrow {}^6\text{A}_1$ ) with a red shift of 10–15 nm. At the present Mn content level ( $\sim 0.2$ ), the red shift can be ascribed to the formation of  $\text{Mn}^{2+}$  pairs.<sup>28</sup> The half-widths of the emission peaks (0.24 eV) indicate that the inhomogeneous broadening is not obvious; that is,  $\text{Mn}^{2+}$  ions have homogeneous coordinate environments. The emission intensities increase monotonically from 7.0 ( $\text{L} = \text{en}$ ) to 54 ( $\text{L} = \text{hda}$ ), which can be attributed to the lengthening of diamine molecules because the Mn contents are approximately identical. It appears that the longer the diamine molecules (the more distant from each other the  $[\text{Zn}_{1-x}\text{Mn}_x\text{Se}]$  monolayers), the stronger the intensities become.

The luminescence-enhancement effect has been studied in the  $\text{CdS}-\text{N}(\text{C}_2\text{H}_5)_3$  and  $\text{Cd}_3\text{As}_2-\text{N}(\text{C}_2\text{H}_5)_3$ <sup>29</sup> colloids and ZnS-en-MCM-41 mesoporous nanosized composites.<sup>30</sup> Triethylamine ( $\text{N}(\text{C}_2\text{H}_5)_3$ ) acts as a donor to enhance the PL intensities by

dramatically lowering the nonradiative decay in  $\text{CdS}$  and  $\text{Cd}_3\text{As}_2$  colloids.<sup>29</sup> Diamines are Lewis bases for  $\text{Zn}^{2+}$  and  $\text{Mn}^{2+}$  ions, which can also act as electron donors to reduce the nonradioactive decay. In the lattices of  $\text{Zn}_{1-x}\text{Mn}_x\text{Se} \cdot 0.5\text{L}$ , all the Zn/Mn ions are linked by the orderly intercalated diamine molecules and form distorted tetrahedra  $\text{Zn/MnNSe}_3$  with Zn/Mn–N bonds (2.16/2.18 Å<sup>15</sup>). Compared with the interaction between  $\text{CdS}$  or  $\text{Cd}_3\text{As}_2$  nanoparticles and  $\text{N}(\text{C}_2\text{H}_5)_3$  molecules capped at their surface, the formation of Zn/Mn–N bonds is more effective on the enhancement of PL intensities.

Furthermore, diamines are also spacers for  $[\text{Zn}_{1-x}\text{Mn}_x\text{Se}]$  DMS layers. The luminescence process, including the energy transfer of excited electron/hole pairs into  $\text{Mn}^{2+}$  ions and a subsequent efficient radiative recombination of the 3d electron, are confined in the 2D DMS layers, which are similar to those in quantum wells or superlattices. When the diamine molecules become longer, the interlayer distances of  $[\text{Zn}_{1-x}\text{Mn}_x\text{Se}]$  layers increase and the interaction between DMS layers is weakened, and the 2D-confined character of the PL process becomes more prominent, which undoubtedly contributes to the luminescence-enhancement effect (as shown in Figure 3). Certainly, more detailed research is needed to verify this deduction.

#### 4. Conclusion

In summary, 2D-DMS  $\text{Zn}_{1-x}\text{Mn}_x\text{Se} \cdot 0.5\text{L}$  ( $\text{L} = \text{diamines}$ ) and their host compounds  $\text{ZnSe} \cdot 0.5\text{L}$  were prepared by solvothermal reaction in solvent  $\text{L}$  at 190 °C. They are isomorphous orthorhombic crystals with almost identical intralayer structures ( $\text{Zn/MnNSe}_3$  coordination tetrahedra) and different interlayer distances of  $[\text{Zn}_{1-x}\text{Mn}_x\text{Se}]$  layers. The orthorhombic lattice in the  $ab$  plane of  $\text{ZnSe} \cdot 0.5\text{en}$  is a shrunk  $\sqrt{3}a \times c$  2D superlattice of the (110) plane of hexagonal ZnSe. A strong  $\text{Mn}^{2+}$ -related emission peak at 600 nm is found in the PL spectra of  $\text{Zn}_{1-x}\text{Mn}_x\text{Se} \cdot 0.5\text{L}$  at room temperature. The Mn content ( $x$ ) dependence of the PL intensities of  $\text{Zn}_{1-x}\text{Mn}_x\text{Se} \cdot 0.5\text{hda}$  are especially researched, and the maximum of PL intensities can be obtained when  $x < 0.2$ . For  $x \approx 0.2$ , the PL intensities of  $\text{Zn}_{1-x}\text{Mn}_x\text{Se} \cdot 0.5\text{L}$  increase monotonically with the lengthening of the diamine molecules. This luminescence-enhancement effect can be ascribed to the formation of Zn/Mn–N bonds and the 2D character of the PL process in the  $[\text{Zn}_{1-x}\text{Mn}_x\text{Se}]$  layers. Our results indicate that  $\text{Zn}_{1-x}\text{Mn}_x\text{Se} \cdot 0.5\text{L}$  are 2D DMS with strong  $\text{Mn}^{2+}$ -related luminescence whose structural, optical, and other properties are worth investigating further due to their unique 2D structural characteristics.

**Acknowledgment.** This work was supported by the National Natural Science Foundation of China, and the National Key Fundamental Research and Development Program of China (973 Program).

#### References and Notes

- (1) Furdyna, J. K. *J. Appl. Phys.* **1988**, *64*, R29.
- (2) Alonso, R. G.; Suh, E.-K.; Ramdas, A. K.; Samarth, N.; Luo, H.; Furdyna, J. K. *Phys. Rev. B* **1989**, *40*, 3720.
- (3) Goede, O.; Heimbrodt, W. *Phys. Stat. Sol. (b)* **1988**, *146*, 11.
- (4) Bartholomew, D. U.; Furdyna, J. K.; Ramdas, A. K. *Phys. Rev. B* **1986**, *34*, 6943.
- (5) Oh, E.; Bartholomew, D. U.; Ramdas, A. K.; Furdyna, J. K.; Debska, U. *Phys. Rev. B* **1988**, *38*, 13, 183.
- (6) Dai, N.; Luo, H.; Zhang, F. C.; Samarth, N.; Dobrowolska, M.; Furdyna, J. K. *Phys. Rev. Lett.* **1994**, *67*, 3824.
- (7) Jonker, B. T.; Liu, X.; Chou, W. C.; Petrou, A.; Warnock, J.; Krebs, J. J.; Prinz, G. A. *J. Appl. Phys.* **1991**, *69*, 6098.
- (8) Kolodziejewski, L. A.; Gunshor, R. L.; Bonsett, T. C.; Venkatasubramanian, R.; Datta, S. *Appl. Phys. Lett.* **1985**, *47*, 169.
- (9) Bylsma, R. B.; Kossut, J.; Becker, W. M.; Kolodziejewski, L. A.; Gunshor, R. L.; Frohne, R. *J. Appl. Phys.* **1987**, *61*, 3011.

- (10) Jin, C.; Zhang, B.; Ling, Z.; Wang, J.; Hou X.; Segawa, Y.; Wang X. *J. Appl. Phys.* **1997**, *84*, 5148.
- (11) Wang, X. Z.; Chen, X.; Liu, J. Z.; Chen, C. J.; Wang, J.; Ling, Z.; Wang, X.; Wang, S. M.; Lu S. Z. *Solid State Commun.* **1995**, *95*, 525.
- (12) Bacher, G.; Schömig, H.; Weisch, M. K.; Zaitsev, S.; Kulakovskii, V. D.; Forchel, A.; Lee, S.; Dobrowolska, M.; Furdyna, J. K.; König, B.; Ossau, W. *Appl. Phys. Lett.* **2001**, *79*, 524.
- (13) Suyver, J. F.; Wuister, S. F.; Kelly, J. J.; Meijerink, A. *Phys. Chem. Chem. Phys.* **2000**, *2*, 5445.
- (14) Huang, X.; Li, J. *J. Am. Chem. Soc.* **2000**, *122*, 8789.
- (15) Huang, X.; Li, J. *Chem. Mater.* **2001**, *13*, 3754. Therein, the reported lattice constants of ZnSe-0.5en single crystal were  $a = 6.6326(7)$ ,  $b = 6.4630(6)$ ,  $c = 17.3540(16)$  Å; those of ZnSe-0.5pda single crystals were  $a = 19.9731(18)$ ,  $b = 6.6268(7)$ ,  $c = 6.4394(6)$  Å.
- (16) Heuling IV, H. R.; Huang, X.; Li J.; Yeun, T.; Lin, C. L. *Nano Lett.* **2001**, *1*, 521.
- (17) Visser, J. W. *J Appl. Crystallogr.* **1969**, *2*, 89.
- (18) Werner, P.-W. *Z. Kristallogr.* **1964**, *120*, 375.
- (19) Werner, P.-W.; Eriksson, L.; Westdahl, M. *J. Appl. Crystallogr.* **1985**, *18*, 367.
- (20) Louer, D.; Louer, M. *J. Appl. Crystallogr.* **1972**, *5*, 271.
- (21) Boulitif, A.; Louer, D. *J. Appl. Crystallogr.* **1991**, *24*, 987.
- (22) De Wolff, P. M. *J. Appl. Crystallogr.* **1968**, *1*, 108.
- (23) De Wolff, P. M. *J. Appl. Crystallogr.* **1972**, *5*, 243.
- (24) Smith, G. S.; Snyder, R. L. *J. Appl. Crystallogr.* **1979**, *12*, 60.
- (25) Deng, Z. X.; Wang, C.; Sun, X. M.; Li, Y. D. *Inorg. Chem.* **2002**, *41*, 869.
- (26) Waldmann, H.; Benecke, C.; Busse, W.; Gumlich, H.-E.; Krost, A. *Semicond. Sci. Technol.* **1989**, *4*, 71.
- (27) Crabtree, D. F. *Phys. Status Solidi A* **1974**, *22*, 543.
- (28) Ronda, R. C.; Amrein, T. *J. Lumin.* **1996**, *69*, 245.
- (29) Dannhauser, T.; O'Neil M.; Johansson, K.; Whitten, D.; Mclendon, G. *J. Phys. Chem.* **1986**, *90*, 6074.
- (30) Zhang, W.; Shi, J.; Chen, J. H.; Hua, Z.; Yan, D. S. *Chem. Mater.* **2001**, *13*, 648.